J Neurophysiol 90: 1392–1407, 2003.
First published May 21, 2003; 10.1152/jn.01049.2002.

A Comparison of Macaque Behavior and Superior Colliculus Neuronal Activity to Predictions From Models of Two-Choice Decisions

Roger Ratcliff, Anil Cherian, and Mark Segraves
Departments of Psychology and Neurobiology and Physiology, Northwestern University, Evanston, Illinois 60208

Submitted 20 November 2002; accepted in final form 19 May 2003

Ratcliff, Roger, Anil Cherian, and Mark Segraves. A comparison of macaque behavior and superior colliculus neuronal activity to predictions from models of two-choice decisions. *J Neurophysiol* 90: 1392–1407, 2003. First published May 21, 2003; 10.1152/jn.01049.2002. Recently, models in psychology have been shown capable of accounting for the full range of behavioral data from simple two-choice decision tasks: mean reaction times for correct and error responses, accuracy, and the reaction time distributions for correct and error responses. At the same time, recent data from neural recordings have allowed investigation of the neural systems that implement such decisions. In the experiment presented here, neural recordings were obtained from superior colliculus prelude/buildup cells in two monkeys while they performed a two-choice task that has been used in humans for testing psychological models of the decision process. The best-developed psychological model, the diffusion model, and a competing model, the Poisson counter model, were explicitly fit to the behavioral data. The pattern of activity shown in the prelude/buildup cells, including the point at which response choices were discriminated, was matched by the evidence accumulation process predicted from the diffusion model using the parameters from the fits to the behavioral data but not by the Poisson counter model. These results suggest that prelude/buildup cells in the superior colliculus, or cells in circuits in which the superior colliculus cells participate, implement a diffusion decision process or a variant of the diffusion process.

INTRODUCTION

A common goal of psychological behavioral research and neurophysiological research is to understand the processes involved in making simple decisions. In psychology, well-established models account for behavioral data from humans executing simple two-choice tasks. Information is assumed to build up over tens or hundreds of milliseconds toward one of two decision criteria, and differences in the rate of build up correspond to differences in decision times between experimental conditions. However, with behavioral data, it is impossible to directly observe the accumulation of information within the decision process. In neurobiology, recordings from single cells in the frontal eye field (FEF) and the superior colliculus (SC) of macaque monkeys have been used to examine simple decision making. Activity in movement-related neurons in the FEF and prelude/buildup cells in the SC has been found to correspond to behavioral eye-movement decisions (Glimcher and Sparks 1992; Gold and Shadlen 2000; Hanes and Schall 1996; Horwitz and Newsome 1999, 2001; Kim and Shadlen 1999; Krauzlis and Dill 2002; Sparks 1999), but to date, there has been no explicit comparison of the dynamics of the decision process inferred from models fitted to behavioral data to the dynamics observed in single cell data.

In this article, we present rhesus monkey behavioral and neurophysiological data from an experimental paradigm almost identical to that used in human experimental psychology. The behavioral data are fit with two models of the decision process, the diffusion model of Ratcliff (Ratcliff 1978, 1981, 1988; Ratcliff and Rouder 1998, 2000; Ratcliff et al. 1999; see also Busemeyer and Townsend 1993; Roe et al. 2001; Smith 1995) and the Poisson counter model (LaBerge 1994; Pike 1966, 1973; Smith and Van Zandt 2000; Townsend and Ashby 1983). If the prelude/buildup cells implement the decision process postulated by either of these models, or are driven by the output from an earlier system that implements the decision process, the cells' activities should be closely related to the dynamics of processing in the model (cf., Ratcliff 1988). In this article, we compare neural firing rates to the average of many simulated paths of evidence accumulation for the diffusion process and the Poisson counter process using parameters obtained from fits to the behavioral data. We find that collicular prelude/buildup activity closely follows the trajectory of the diffusion model's decision process but not the decision process of the Poisson counter model.

METHODS

Two female adult rhesus monkeys (*Macaca mulatta*), each weighing 8 kg, were used for these experiments. Northwestern University's Animal Care and Use Committee approved all procedures for training, surgery, and experiments performed with these monkeys. Each monkey received preoperative training followed by an aseptic surgery to implant a subconjunctival wire search coil, a stainless steel recording cylinder aimed at the superior colliculus, and a stainless steel receptacle to allow the head to be held still during behavioral and neuronal recordings. All of these methods have been described in detail elsewhere (Dias and Segraves 1999; Segraves 1992). Surgical anesthesia was induced with the short-acting barbiturate Brevital (11 mg/kg) injected through an intravenous line and maintained using halothane (1%) inhaled through an endotracheal tube. Our neuronal recordings focused on neurons with preparatory and saccade-related activity in the deep layers of the SC. In this report, we define deep layers as all collicular layers located below the superficial layers (superficial gray and stratum opticum), including the intermediate and deep gray layers. Assurance that the neurons included in this study were confined

Address for reprint requests: R. Ratcliff, Dept. of Psychology, Ohio State University, 1827 Neil Ave., Columbus, OH 43210.

The costs of publication of this article were defrayed in part by the payment of page charges. The article must therefore be hereby marked "*advertisement*" in accordance with 18 U.S.C. Section 1734 solely to indicate this fact.

to the deep layers of the SC is based on the fit of our electrode penetrations to the highly reproducible map of the SC, the ability to evoke saccades from our recording sites with current intensities of $<50\ \mu$A, and the match of recorded activity to established cell activity types in these layers (Cynader and Berman 1972; Mays and Sparks 1980; Munoz and Wurtz 1995; Robinson 1972).

Neural firing rates were recorded within the deep layers of both the left and right SC of both monkeys (identified as MK03 and MK07). A total of 90 cells were classified into three categories, prelude/buildup cells, burst cells, and visuomovement cells, based on conventional oculomotor tasks, i.e., the contribution of visual-related, delay period-related, and movement-related activities to their firing patterns. The focus of this research was on the behavior of the prelude/buildup cells (Glimcher and Sparks 1992; Mohler and Wurtz 1976; Munoz and Wurtz 1995; Sparks et al. 1976), which were identified with a gap saccade task. In the gap task, the monkey fixated on a light that disappeared after 1–2 s; after a delay of $\leq$400 ms, a peripheral target was turned on. Neurons with prelude/buildup activity increased their firing rates during this gap period in anticipation of the appearance of the target light. The activities of the prelude/buildup cells were recorded while the monkey performed the two-choice task described below.

Experimental task

In research in which single cell recordings are obtained in monkeys, the stimulus and response often have a strong spatial correspondence. For example, in a stimulus detection task, a single light is presented with the required response an eye movement to it (Hanes and Schall 1996). The spatial location of the light is the same location as the target of the saccade. In a visual search task, several dots are arranged in a circle, and when one of them changes color, the required response is a saccade to the location of the dot changing color (Bichot et al. 2001; Schall et al. 1995; Thompson et al. 1996). In motion detection tasks in which stimuli consist of moving dots with a proportion moving in random directions and remaining dots moving in a particular direction, the required response is an eye movement in the direction of motion (Horwitz and Newsome 1999; Kim and Shadlen 1999). With tasks like these, it is possible that the eye movement response could be primed by visual information from the stimulus: information from the visual representation of the stimulus could flow straightforwardly, without transformation, through to the FEF or SC where the response is initiated (e.g., Sato et al. 2001). To avoid the possibility of such priming, the task we used decouples the stimulus and the response. The stimuli are lights arranged in a vertical display and the required response is not an eye movement to one of these lights but instead an eye movement to a target light presented horizontally to the left or right. In this task, the response is decoupled from the stimulus which means that it is not possible for a response to be primed early in the time course of the decision by information being mapped from earlier visual representations of the stimulus directly to later visual output representations; the stimulus information has to be transformed from the stimulus representation to the response representation. The other requirement of the task was that it was one that had been used in the human literature and one that we knew could be successfully fit by sequential sampling models (e.g., Ratcliff and Smith 2003; Ratcliff et al. 2001).

The task we used was a two-choice task in which the monkey decided whether the distance between a test stimulus light and a fixation light was small or large (Fig. 1). To indicate their responses, the monkeys were trained to make a saccade to one of two response target lights: one in the left visual hemifield for a "small" response and the other in the right hemifield for a "large" response. The response target lights were adjusted for each cell from which we recorded by placing one response target light in the center of the cell's receptive field and the other response target light at the mirror-symmetrical position in the opposite hemifield. The fixation light was always

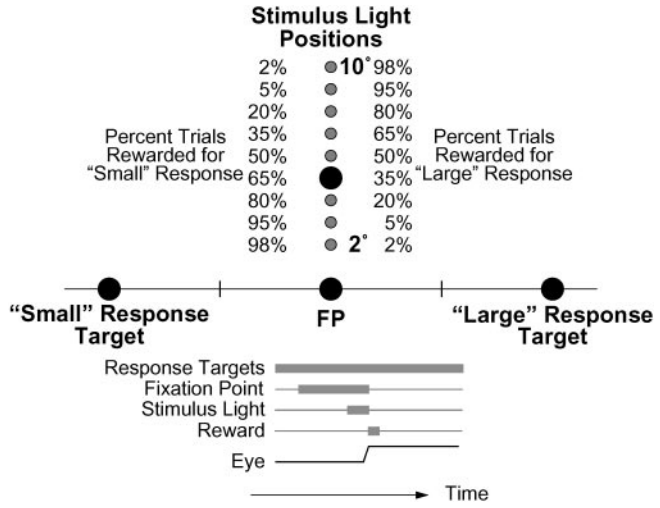

FIG. 1. Behavioral task. The monkey was presented with a fixation point on the screen (FP), and the stimulus light was illuminated. It could occur in any 1 of the 9 positions (small shaded circles) located from 2° to 10° from the fixation point. In this example, the stimulus light (large filled circle above the fixation point) is positioned 5° from the fixation point. The task of the monkey was to move its eyes to 1 of the 2 target lights that were illuminated through the whole trial. Target lights were not in fixed positions, but were moved so that one fell in the center of the receptive field of the cell. Probability of reinforcement is shown next to the stimulus light position. Time course of the onset of the fixation point, stimulus lights, reinforcement, and saccade are shown at the bottom of the figure.

presented at the center of the display screen. The test stimulus light was positioned vertically above or below the fixation light, with its distance from the fixation light varied randomly from trial to trial over a range of 2–10° in 1° increments. Feedback varied as a function of distance so that a "large" response to the middle distance (6°) was rewarded with probability 0.5, a "large" response to the largest distance (10°) was rewarded with probability 0.98, and so on (see Fig. 1). This task is similar to ones that examine probability matching (see Ratcliff et al. 1999) and is also the one-dimensional analog of tasks that are used in testing models of categorization behavior. The two dominant models are distance from the criterion models (e.g., Ashby 2000) and exemplar based models (e.g., Nosofsky and Palmeri 1997). In fact, variants on this task have been used to test between these models of categorization in humans (Rouder and Ratcliff 2003) and in monkeys (S. Farrell, R. Ratcliff, A. Cherian, and M. A. Segraves, unpublished observations).

The distance/reward probability manipulation was designed to vary difficulty, with responses to test stimuli that were near or far from the fixation light easy and responses to middle distance stimuli difficult. Because of the variable feedback, the monkeys could not be perfectly correct in their responses. Note that in this article, we use the term "error" as shorthand to refer to "small" responses to "large" stimuli and "large" responses to "small" stimuli. The large and small response target lights were kept on throughout the running of the task. The fixation point appeared at the beginning of each trial, and after the monkey achieved fixation, the fixation point remained illuminated for a randomly varied interval of 500–1,500 ms. At the end of this interval, the test stimulus light was turned on. Test stimulus light and fixation point then remained on for $\leq$5,000 ms while the monkey was given the opportunity to make a saccade to one of the response target lights. Trials with saccades made to either response target light were scored as valid and included in the data used for this report, regardless of whether the saccade was rewarded or not. Trials on which the monkey failed to make a saccade, made a saccade that did not terminate at either response target, or made a saccade in under 120 ms were rejected. Reaction times (measured from stimulus onset to start of the saccade), response choices, and cell activities were recorded

while the monkey performed the task for approximately 60–90 min for each recording session, with one recording session for each cell.

The neural activity and behavioral data for a cell were included in the data analyses only if there was a minimum of 300 trials for the cell on which the monkey made a saccade to one of the response target lights. Thirty-seven cells in our sample were classified as having prelude/buildup activity. Sufficient data to include in the analyses were collected from 28 of them. In MK03, 10 were recorded in the right colliculus and 9 in the left colliculus, and in MK07, 3 were recorded in the right colliculus and 6 in the left colliculus. Trials were excluded if the saccade duration was <10 or >100 ms, if the reaction time was <120 ms (e.g., Swensson 1972), or if the reaction time was >900 ms (these latter 2 limits excluded <0.8 and 0.4% of the data for monkeys MK03 and MK07, respectively). We collected a total of 15,453 trials with ≥ 300 trials per session per cell.

Diffusion model

The diffusion model is designed to apply only to two choice decisions that are relatively fast and composed of a single-stage decision process (as opposed to the multiple-stage decision processes that might be involved in, for example, reasoning or problem solving tasks). As a rule of thumb, the model would not be applied to experiments in which mean reaction times are much longer than about 1–1.5 s.

The diffusion model assumes that decisions are made by a noisy process that accumulates information over time from a starting point toward one of two response criteria or boundaries, as in Fig. 2, where the starting point is labeled *z* and the boundaries are labeled *a* and 0. When one of the boundaries is reached, a response is initiated. The rate of accumulation of information is called the drift rate (v), and it is determined by the quality of the information extracted from the stimulus. For example, if the stimulus with a large separation between the two dots was displayed, information quality toward a "large" response would be good and the value of the drift rate toward the "large" boundary would be large. Within each trial, there is noise (variability) in the process of accumulating information so that processes with the same mean drift rate do not always terminate at the same time (producing reaction time distributions) and do not always terminate at the same boundary (producing errors). This source of variability is called "within trial" variability and has SD s. This parameter is not estimated in fitting; it is a scaling parameter and is set to $s = 0.1$; if its value was doubled, other parameters of the model could be doubled to produce exactly the same predictions.

Empirical reaction time distributions are positively skewed. The diffusion model naturally predicts this shape by simple geometry, as shown in Fig. 2. The differences in drift rate between the middle arrow and the other two arrows starting at *z* in Fig. 2 have equal size, and these map into a skewed distribution on the top boundary (equal vertical differences map onto unequal horizontal differences). Accounting for differences in reaction time between correct and error responses has long been a problem (see Luce 1986), but in the diffusion model, the relative speeds of correct and error responses can be explained by assuming variability in components of processing across trials. Variability in drift rate across trials leads to slow errors and variability in starting point leads to fast errors (see Ratcliff and Rouder 1998; Ratcliff et al. 1999).

Besides the decision process, there are nondecision components of processing such as encoding and response execution. These are combined in the diffusion model into one parameter, T_{er}. Like drift rate and starting point, T_{er} is assumed to be variable across trials and is assumed to have a uniform distribution with range s_t (see Ratcliff and Tuerlinckx 2002; Ratcliff et al. 2003). Because the SD in the distribution of T_{er} is typically less than one-quarter the SD in the decision process, the combination of the uniform distribution of T_{er} and the diffusion process distribution (their convolution) produces a reaction time distribution almost identical to the diffusion process distribution

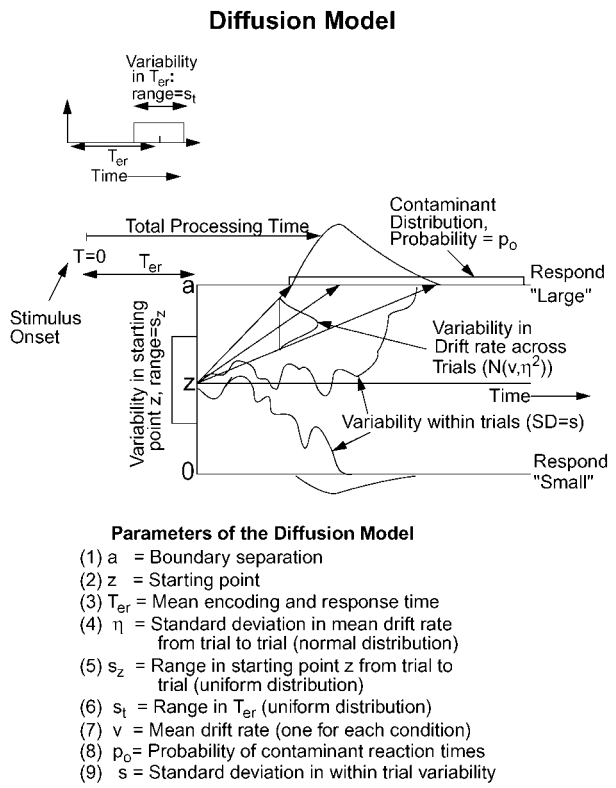

FIG. 2. Diffusion model. Evidence is accumulated from a starting point *z* toward response boundaries at 0 and *a*. Rate of accumulation of information, drift rate (v), is noisy; it varies around its mean so that processes with the same mean drift rate can reach the same boundary at different times or reach different boundaries (leading to correct and error responses). Variability within a trial is represented by a parameter *s*, which is a scaling parameter (if it is doubled, other parameters of the model can be doubled to give exactly the same fits), and it is set to a value 0.1. Drift rate for an experimental condition represents the rate of accumulation of evidence. In this experiment, drift rate is a function of the distance between fixation point and stimulus light. The speed and accuracy of a decision are a function jointly of the drift rate and the distances of the response boundaries from the starting point. Speed-accuracy trade-offs, frequently observed in human data, occur when the boundaries are moved farther apart to produce slower and more accurate responses or closer together to produce faster and less accurate responses. Processes involved in a response other than the decision process itself are represented by a time parameter (T_{er}). Variability is assumed in drift rate (normal distribution with SD η), starting point (uniform distribution, range s_z), and the duration of other processes (uniform distribution, range s_t, e.g., $s_t = 60$ ms has SD $60/\sqrt{12} = 17$ ms). Contaminant reaction times are represented as a uniform distribution with range between the minimum and maximum reaction times and the proportion of contaminant reaction times is represented by a parameter (p_o).

(see Ratcliff and Tuerlinckx 2002, their Fig. 11). Variability in T_{er} stretches out the leading edge of the reaction time distribution, stretching the difference between the 0.1 and 0.3 quantiles (the reaction time at which 0.1 and 0.3 of the processes have terminated, respectively) by typically $<10\%$ of s_t.

In summary, the parameters of the diffusion model correspond to the components of the decision process as follows: *z* is the starting point of the accumulation of evidence, *a* is the upper boundary, and the lower boundary is set to 0. The amount of variability in the mean drift rate across trials is assumed to be normally distributed with SD η and the variability in starting point is assumed to have a uniform distribution with range s_z. For each stimulus condition in an experiment, it is assumed that the rate of accumulation of evidence is different and so each has a different value of drift, v. Within-trial variability in drift rate (s) is a scaling parameter for the diffusion process and is fixed at a value 0.1.

Poisson counter model

Our main aim in fitting the Poisson counter model to the behavioral data and examining its predictions for the buildup of discriminative information in the decision process is to provide a plausible alternative model that makes predictions different from the diffusion model. It turns out that the Poisson counter model does not fit the behavioral data as well as the diffusion model, and produces some significant discrepancies between predictions and data. It also predicts a qualitatively different pattern for the buildup of discriminative information in the decision process than the diffusion model.

The Poisson counter model assumes that evidence is accumulated in two counters, one for each response alternative (LaBerge 1994; Pike 1966, 1973; Smith and Van Zandt 2000; Townsend and Ashby 1983). Evidence is accumulated in discrete unit counts toward a different decision criteria for each response. The units of evidence arrive at exponentially distributed times (as opposed to earlier counter models in which evidence arrived at discrete time steps, e.g., LaBerge 1962; see also, Ratcliff and Smith 2003). We chose this model because it is representative of the class of two counter models, because it has some neural plausibility because spike trains can be modeled as Poisson processes, and because it is a competitor for the diffusion model (see Ratcliff and Smith 2003; Van Zandt et al. 2000).

Figure 3 illustrates the model and shows the model's parameters. Figure 3, *top*, shows the arrival times of counts at the two counters, one for "large" responses and the other for "small" responses, and Fig. 3, *bottom*, shows the accumulation of counts in the two counters. The interarrival times (the "accrual rates") are exponentially distributed with rate parameter α for counter A and rate parameter β for counter B. With exponentially distributed interarrival times, the processes are Poisson processes, and the mean interarrival times are therefore $1/\alpha$ and $1/\beta$. The accrual rates in the Poisson counter model serve the same function as the drift rates in the diffusion models: an increase in the quality of the information from the stimulus (e.g., greater separation of the stimulus and fixation lights) is mapped to an increase in the accrual rate for the appropriate counter.

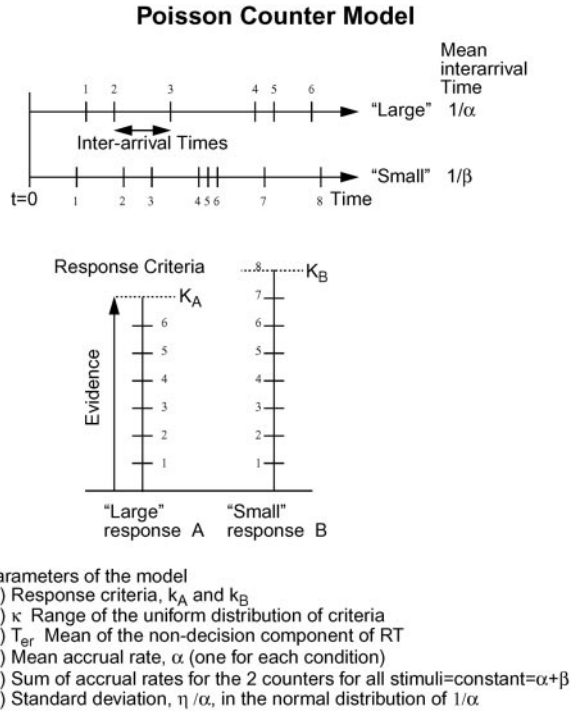

FIG. 3. Poisson counter model. Evidence is accumulated in 2 counters, 1 for each response. Evidence arrives in discrete equal size units at exponentially distributed times. There are 2 response criteria, K_a and K_b, which randomly vary across trials from uniform distributions with means k_a and k_b and with range κ. The rate at which counts are accumulated are α and β, and the sum of these is a constant (another parameter of the model). For a high rate of accumulation, α is increased and β is decreased so $\alpha + \beta$ is a constant. Rate of accumulation is assumed to vary across trials, and we assumed a normal distribution of values based on the time constant (mean time between counts) that was larger the larger the time constant (e.g., η/α). Processes involved in a response other than the decision process itself are represented by a time parameter (T_{er}).

As each count arrives, it is accumulated in the appropriate counter. A response is initiated when one or the other of the counters reaches its criterion value, K_A or K_B. Varying the values of the response criteria allows the model to account for manipulations such as the effects of speed versus accuracy instructions. Nondecision components of processing are summarized in the parameter T_{er}, just as for the diffusion model.

We assume that the sum of the two accrual rates, $\alpha + \beta$, is constant; therefore increasing one of the rates results in a corresponding decrease in the other rate. This constraint means that overall evidence for both alternatives is accumulated at the same rate ($\alpha + \beta$) for each different stimulus. This assumption mirrors the assumption in the diffusion model that s, which controls the rate at which a process diffuses toward its boundaries, remains constant, while mean drift rate varies with stimulus difficulty. The parameter α is free to vary across experimental conditions, but the sum $\alpha + \beta$ is fixed across experimental conditions.

Two sources of across-trial variability are assumed for the Poisson counter model. First, across-trial variability in accrual rates was implemented as follows: we assumed variability in the time constant derived from the rate parameter α, i.e., $\tau = 1/\alpha$. This variability was assumed to be normally distributed with SD a proportion, η, of $1/\alpha$, i.e., $\eta\tau$. Because the sum of $\alpha + \beta$ is constant, this produces corresponding variability in β.

The second source of across-trial variability comes from variability in the response criteria. For each criterion, we assume a rectangular distribution with the same range κ. The criteria are discrete numbers so the mean and range of the rectangular distribution define a probability mixture of integer criterion values. In fits to the data, the range was small, and there were only two values in the mixture for each of the criteria for each of the monkeys.

Just as for the diffusion model, a parameter T_{er} represents processes other than the decision process. In the application of the Poisson counter model here, it was not necessary to include a parameter for variability in T_{er}. Fits of the Poisson counter model in Ratcliff and Smith (2003) showed that allowing variability in T_{er} did not improve fits of the model. Adding variability in T_{er} has the effect of stretching out the leading edge of the reaction time distribution, and in the data presented by Ratcliff and Smith, the leading edge was either adequately predicted or overpredicted. In the fits to the data presented below, the spread in the leading edge is overpredicted by the Poisson counter model with T_{er} fixed (i.e., $s_t = 0$).

Presentation of behavioral results

The behavioral data consists of the probabilities of "large" versus "small" responses and the reaction time distributions for those responses for each of the stimulus conditions (distances). The behavioral results are displayed in pairs of quantile probability functions. In these, data from "small" and "large" responses are plotted separately. Data for each stimulus or group of stimuli are used to produce reaction time quantiles and these are plotted vertically on the *y*-axis and their location on the *x*-axis is the probability of the "small" or "large" response. This method of presenting data was developed by Ratcliff (2002) to allow response probability and the shapes of the reaction time distributions for correct and "error" responses to be all displayed in one plot and allow visualization of how the different dependent variables covary.

Figure 4 illustrates how reaction time distributions can be derived from quantile reaction times. In the examples shown in Fig. 4, because

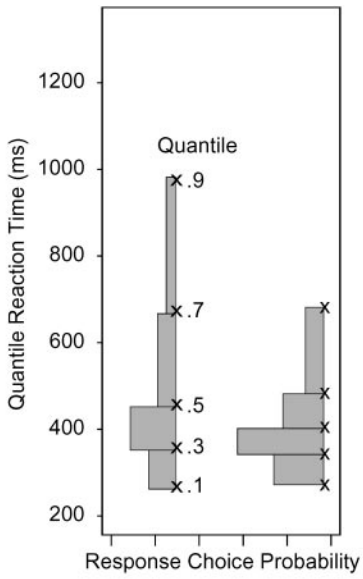

FIG. 4. Relationship between reaction time quantiles and distributions. Two sets of 5 reaction time quantiles are plotted, and equal area rectangles are drawn between the quantiles to represent reaction time distributions.

there is 0.2 probability between each of the quantiles, equal area rectangles can be drawn between the quantiles (see Ratcliff 1979) to produce reaction time distributions. The two distributions illustrate what happens when the change in mean reaction time involves little change in the 0.1 quantile and larger changes in the higher quantiles: the reaction time distribution skews.

RESULTS

Figure 5 shows plots of the probability of a "large" response for the data and for predictions from the fits of the diffusion model to the data (the psychometric function). Figure 5, *bottom*, shows fits of mean reaction time to the data; the error bars are ±2 SE. Most of the predicted reaction times lie within 2 SE.

Figure 6 shows quantile probability plots for the data from "small" responses (*left*) and "large" responses (*right*) for the two monkeys. The experimental data for the extreme conditions (2–3 and 8–10°) were almost the same, so we grouped these extremes to reduce the nine experimental conditions to six (Fig. 6, *A–F*). Probability of a "large" or "small" response is plotted on the *x* axis, so, for example, for the *top left panel* for group A, the probability of a "small" response was over 0.99, and for group C in the *top right panel*, the probability of a "large" response was about 0.3. To construct these plots, the 0.1, 0.3, 0.5 (median), 0.7, and 0.9 quantile reaction times for "large" and "small" responses for each experimental condition were computed. These represent the reaction times at which 0.1, 0.3, etc. of the responses have terminated. To help orient, the data for the middle distance stimulus (6°, labeled group D) are indicated by a gray rectangle. There were too few responses (e.g., only 7 or 8) in the lowest probability conditions to produce reliable estimates of reaction time quantiles, so only five columns of data (crosses) are shown.

The results show the following trends for which the behavioral model must account (all of which are obtained in human data, see Ratcliff et al. 2001). First, reaction time distributions are skewed toward longer reaction times. This is shown by greater separation between the higher quantile reaction times than the lower quantile reaction times. Second, the more difficult conditions (B and C for "small" responses and D and E for "large" responses in Fig. 6) have longer reaction times and lower response probabilities than the easier conditions (A for "small" responses and F for "large" responses in Fig. 6). Third, "small" responses to "large" stimuli and "large" responses to "small" stimuli have longer response times than "large" responses to "large" stimuli and "small" responses to "small" stimuli. Fourth, as reaction time increases from easier to harder conditions, most of the change in reaction time is in the distribution skewing rather than shifting; there is little change in the 0.1 quantiles across response probabilities and there are larger changes in the higher quantiles (e.g., condition A vs. condition C for "small" responses in Fig. 6).

Fits of the diffusion model to behavioral data

The diffusion model was fit to the data using a general SIMPLEX minimization routine that adjusts the parameters of the model to find the parameters that give the minimum of a χ^2 goodness of fit measure (see Ratcliff and Tuerlinckx 2002). The data used by the minimization method for each experimental condition were the response times for each of the five quantiles for correct and "error" responses and the accuracy

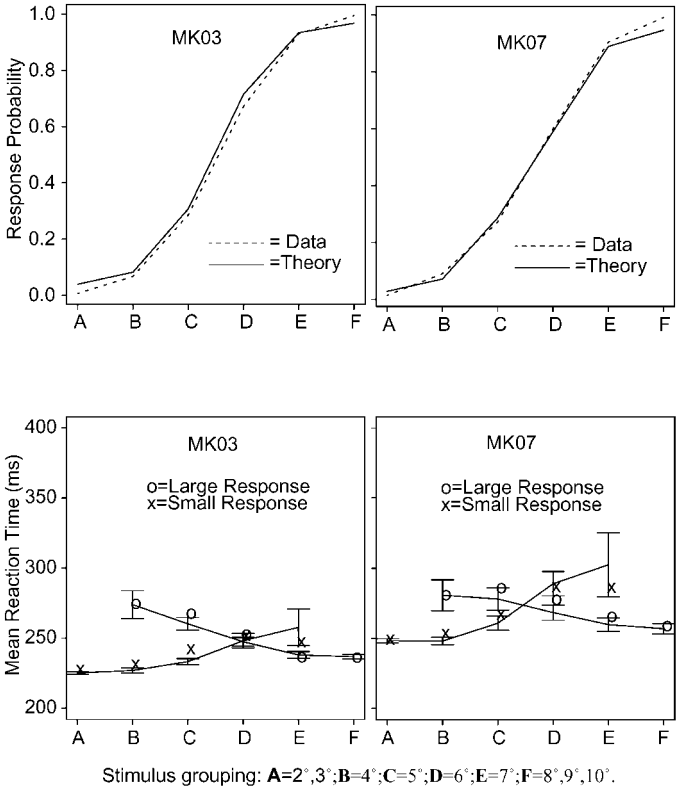

FIG. 5. Fits of diffusion model to accuracy and mean reaction time. Plots are presented for probability of a large response and for mean reaction time for "large" and "small" responses for the data and for predictions from the diffusion model as a function of stimulus condition for the 2 monkeys. Error bars for reaction time are ±2 SE.

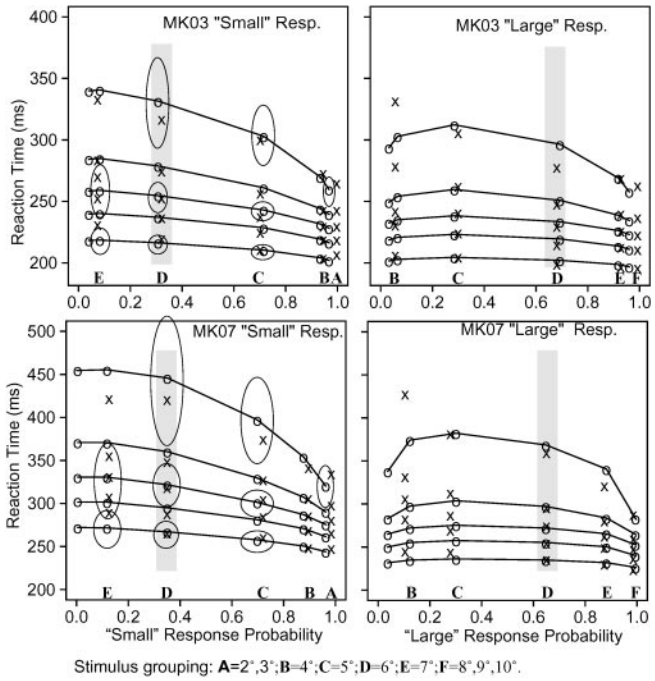

FIG. 6. Fits of the diffusion model to the behavioral data. Diffusion models (fitted values are circles, connected by solid lines) were fit to the behavioral data (crosses). Response probability was computed along with the 0.1, 0.3, 0.5 (median), 0.7, and 0.9 quantile reaction times for "large" and "small" responses for each experimental condition. Quantiles represent the reaction times at which 0.1, 0.3, etc. of the responses have terminated. Experimental conditions were combined into 6 groups, A–F, listed at the *bottom*. Data for the middle distance stimulus (6°) are indicated by a gray rectangle. There were too few responses (e.g., only 7 or 8) in the lowest probability conditions to produce reliable estimates of reaction time quantiles, so only 5 columns of data (crosses) are shown.

values. The observed proportions of responses for each quantile are the proportions of the distribution between successive quantiles (i.e., the proportions between 0, 0.1, 0.3, 0.5, 0.7, 0.9, and 1.0 are 0.1, 0.2, 0.2, 0.2, 0.2, and 0.1). The quantile reaction times were used to produce predicted cumulative probabilities from the diffusion model. For a good fit, these would be close to 0.1, 0.3, etc., but if the fit were poor they would differ from these values. Subtracting the cumulative probabilities for each successive quantile from the next higher quantile gives the predicted or expected proportion of responses between each quantile. For the χ^2 computation, these expected proportions are compared with the observed proportions of responses between the quantiles (multiplied by the number of observations). These probabilities are converted to frequencies to produce the χ^2 value by multiplying them by the response probability for the condition and then by the number of observations. Summing the value of the (Observed − Expected)^2/Expected for all conditions, where observed and expected are frequencies, gives a single χ^2 value to be minimized (see Ratcliff and Tuerlinckx 2002 for a detailed description).

Ratcliff and Tuerlinckx (2002) assumed that some proportion of responses between the short and long cutoffs (120 and 900 ms) were also contaminants and they modeled them by assuming that they arose from a random delay added to the usual decision process. The delay was assumed to vary uniformly between the minimum and maximum reaction time in each condition and there was a common probability of a contaminant across all conditions. This probability adds one additional parameter to the diffusion model (p_o). We fit the diffusion model to the data reported here with the most general fitting program, the one with this contaminant assumption. In the fits presented next, p_o was 0 for MK03 and 0.034 for MK07. The latter value is small, and the fits would be indistinguishable from fits with the proportion set to zero.

For the fits presented here, all parameters were held constant across the six conditions (Fig. 6, *A–F*) except drift rate; changes in accuracy and reaction time distribution shape across conditions were assumed to be accounted for by changes in drift rate. Changes in drift rate change both reaction time and accuracy and a plot of reaction time quantiles against accuracy as drift rate changes produces the solid lines in Fig. 6. Thus changing drift rate moves quantile reaction times horizontally along the quantile probability function, but does not alter the shape of the reaction time distribution (the relative spread of the quantiles is about the same all along the function).

The fits of the model to the behavioral data are shown in Fig. 6 by the horizontal lines and circles and the parameter values are shown in Tables 1 and 2. The ellipses in Fig. 6, *left*, are shown for a sample subset of points and provide approximate 95% confidence regions around the theoretical predictions. These were obtained using a Monte Carlo method (Ratcliff and Tuerlinckx 2002): 40 sets of simulated data were generated using the best fitting parameters of the model. These formed roughly elliptical blobs (confidence intervals) around the theoretical predictions. The ellipses become larger moving from high response probability to low response probability because the number of observations decreases, and the ellipses become larger moving from the 0.1 to the 0.9 quantiles because there is more variability in the tails of the reaction time distribution than in the leading edges. The response probability values and 0.1, 0.3, 0.5, and 0.7 reaction time quantiles derived from the diffusion model fit the data well (within 4% in probability and within 15 ms in reaction time). There were larger discrepancies in the 0.9 quantile (for which the data are more variable), but these were still within the confidence ellipses.

Fits of the Poisson counter model to behavioral data

We fit the Poisson counter model to the experimental data using a weighted least-squares method (see Ratcliff and Smith 2003; Ratcliff and Tuerlinckx 2002). The fits are shown in Fig. 7, and the parameter values are shown in Tables 2 and 3. The first thing to note is that the fits are worse than the fits of the diffusion model. For the data from both monkeys, the model consistently produces predictions that are much larger than the empirical 0.1 quantiles for "small" responses. These discrepancies are highly significant; most fall outside 2 SE, which are about the same as those shown in ellipses in Fig. 7, and for example, the probability of five discrepancies (i.e., 1 at each

TABLE 1. *Diffusion model parameters*

Subject	a	T_{er}, s	η	s_Z	p_o	s_t, s	z
MK03	0.054	0.202	0.491	0.006	0.000	0.051	0.033
MK07	0.064	0.236	0.399	0.017	0.034	0.060	0.043

a, boundary separation; z, starting point, T_{er}, nondecision component of response time; η, SD in drift across trials; s_z, range of the distribution of starting point; p_o, proportion of contaminants; s_t, range of the distribution of nondecision times.

TABLE 2. *Diffusion model drift rates (s^{-1}) and Poisson counter model accrual rates (s^{-1})*

Model	Subject	Stimuli 2, 3	Stimulus 4	Stimulus 5	Stimulus 6	Stimulus 7	Stimuli 8, 9, 10
Diffusion	MK03	−0.94	−0.72	−0.20	0.44	1.03	1.25
Diffusion	MK07	−1.42	−0.50	−0.06	0.23	0.74	0.94
Poisson	MK03	7.35	15.18	22.43	31.90	37.11	37.38
Poisson	MK07	1.07	7.41	16.55	29.07	39.12	33.06

stimulus grouping for the 0.1 quantile) at the 0.05 level is 0.00000031. The model also fails to predict the reduction in reaction time as response probability approaches 1. For both "large" and "small" responses, the 0.9 quantile reaction time is discrepant by 40–50 ms. The predicted quantile probability functions are roughly flat across the range of response probability values, quite different from the diffusion model's inverted U-shaped functions. These failures mean that the model does not fit the data adequately.

Growth of information in firing rate data

We present three analyses of the neural firing data. The first analysis examines firing rates as a function of the probability of the response to a response target light being high, medium, or low. We use the probability of the response to refer to stimulus-response combinations that are similar: the high probability condition corresponds to a stimulus grouping of 2, 3, and 4° targets for a "small" response combined with 7, 8, 9, and 10° targets for a "large" response (dashed lines in Fig. 8). The medium probability condition corresponds to a stimulus grouping of 5 and 6° targets for either response (solid line). The low probability condition corresponds to a stimulus grouping of 2, 3, and 4° targets for a "large" response combined with 7, 8, 9, and 10° targets for a "small" response (dotted line). The second two analyses examine the firing rates for the medium probability conditions and provide functions representing the growth of discriminative information in firing rates. These latter two analyses are target data sets for modeling.

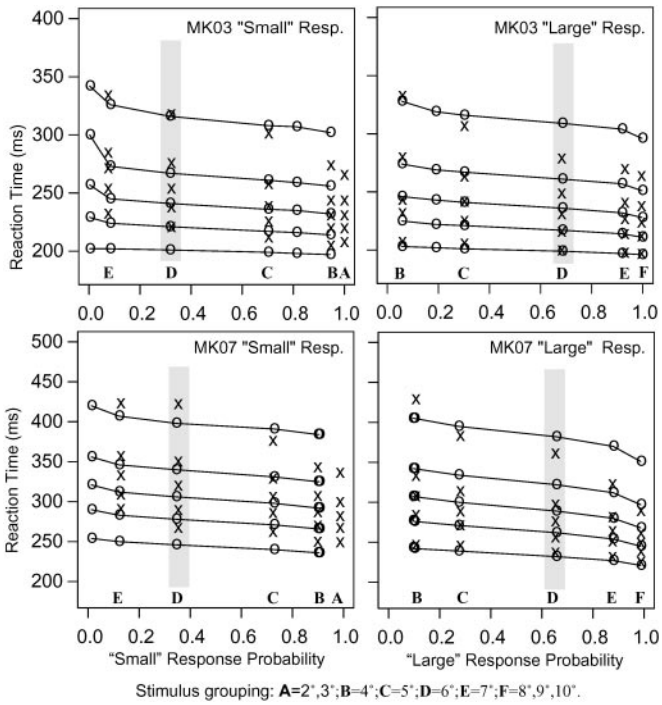

FIG. 7. Fits of the Poisson counter model to the behavioral data. Poisson counter models (predicted values are solid lines) were fit to the behavioral data (crosses), and the conditions correspond to those in Fig. 6.

We present firing rate data averaged over sessions and over the two monkeys for the 28 cells in our sample. The plots all use 8-ms bins, and the functions are not filtered or smoothed. In each analysis, we present firing rate as a function of time for cells that are in the receptive field of the response target to which the saccade response is made and for cells that are in the receptive field of the other response target, i.e., the response target to which the saccade is not made. This allows us to examine the growth of activity in cells when a saccade is made into its receptive field and when a saccade is made to the other response target. The difference between these two firing rates provides the growth of information in firing rate that discriminates between the two responses.

Figure 8*A* shows firing rate functions for saccades into the receptive field of the response target as a function of whether the probability of that response is high, medium, or low. The firing rate functions rise from about the same point with only small differences in the rate of increase that correspond to the relatively small differences in reaction time, and the peak activity of the functions is at about the same firing rate.

Figure 8*B* shows firing rate functions for the receptive field of a response target when the saccade is made to the other response target as a function of whether the probability of that response is high, medium, or low (with the same groupings as in Fig. 8*A*). When the probability is high for a response to the other response target and a response is made to it (Fig. 8*B*, dotted line), the firing rate is small, but when the probability is low for a response to the other response target and a response is made to it (Fig. 8*B*, dashed line), there is a moderate level of activity in the cells (about one-half the peak activity for the functions in Fig. 8*A*). Note that for the low probability conditions, there are few responses and the corresponding firing rate functions are noisy (Fig. 8*A*, dotted line, and Fig. 8*B*, dashed line). The increase in firing rate in Fig. 8*B* from the low to high probability conditions provides evidence for competing activity in the populations of neurons that correspond to the two target lights and this is taken up in the discussion.

The next two analyses divide the firing rate data from the

TABLE 3. *Poisson counter model parameters*

Subject	k_A	k_B	η	κ	T_{er}, s	$\alpha + \beta$
MK03	3.71	3.52	0.312	0.651	0.182	45.0
MK07	4.92	5.93	0.242	0.801	0.190	46.2

k_A and k_B, two decision criteria; rate/η, SD in Poisson rate across trials (see text); T_{er}, non-decision component of response time; κ, range in criterion values; $\alpha + \beta$, sum of Poisson rates for the two counters.

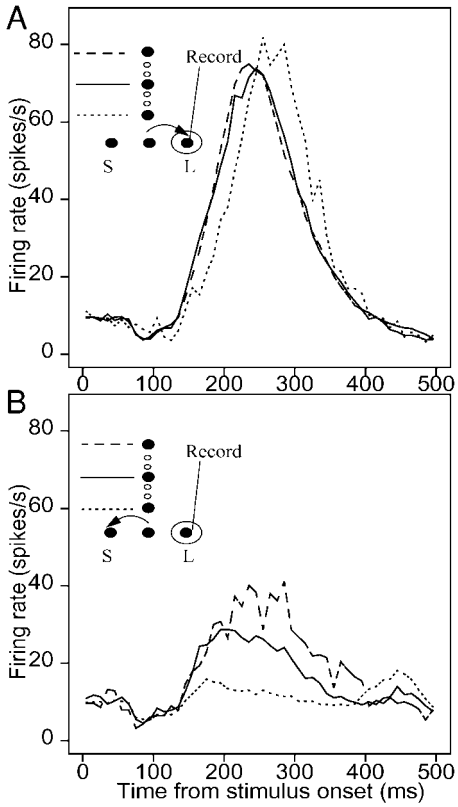

FIG. 8. Neural firing rates for large, medium, and small stimuli. *A*: activity for cells when a saccade is made to the target in the receptive field for "high probability" (probability of a response greater than 0.8), "medium probability" (probability between 0.2 and 0.8), and "low probability" (probability below 0.2) conditions. The high probability condition corresponds to "large" responses to large stimuli (7, 8, 9, and 10°) for recordings in the left colliculus and "small" responses to small stimuli (2, 3, and 4°) for recordings in the right colliculus (dashed lines); for the medium probability condition, "large" responses to the medium stimuli (5 and 6°) for the left colliculus were combined with "small" responses to the medium stimuli for the right colliculus (solid lines); for the low probability condition, "large" responses to small stimuli in the left colliculus were combined with the "small" responses to large stimuli in the right colliculus (dotted lines). There were no significant differences in decisions to small and large stimuli in the left and right colliculi as would be expected if the task produced different results for foveal stimuli (2°) and peripheral stimuli (10°). Number of trials in the figures are as follows: *A*: 189, 1712, and 5334 for the dotted, solid, and dashed lines, respectively; *B*: 5339, 1853, and 220 for the dotted, solid, and dashed lines, respectively. *Inset*: stimuli and response target from which the recording was made; ellipse represents the center of the receptive field of the cell.

medium probability conditions into thirds that correspond to fast, intermediate, and slow responses. Sato et al. (2001) presented this kind of analysis for firing rates in visually responsive cells in the FEF for a visual search task when targets fell in the receptive field of the cell and when they did not (see also Bichot et al. 2001). Their function representing the difference in firing rates for slow responses showed a delayed onset relative to the function for fast responses when the firing rates were aligned on the stimulus (e.g., Sato et al. 2001, their Fig. 3). It might be expected that models that assume a gradual growth of information such as the diffusion model or the Poisson counter model could not produce such a delay in the onset of discriminative information for slow relative to fast responses. When the firing rates were aligned on the saccade, there was no difference in the onset of discriminative information.

We chose to use the intermediate probability targets (stimuli of 5 and 6°) because there are approximately equal numbers of observations for responses to both response alternatives, a total of about 300 trials for each of the six functions. This means that there are enough data to produce smooth firing rate functions with little variability compared with the high and low probability condition data for which there are few observations for responses made to the low probability target.

Figure 9 shows the firing rate functions for fast, intermediate, or slow responses aligned on stimulus onset. Figure 9*A* shows firing rates for saccades into the receptive field of the response target, and Fig. 9*B* shows firing rates for the receptive field of a response target when the saccade is made to the other response target. For saccades into the receptive field of the response target (Fig. 9*A*), the firing rate functions start to rise at about the same point in time and grow more quickly for fast responses than intermediate responses, and more quickly for

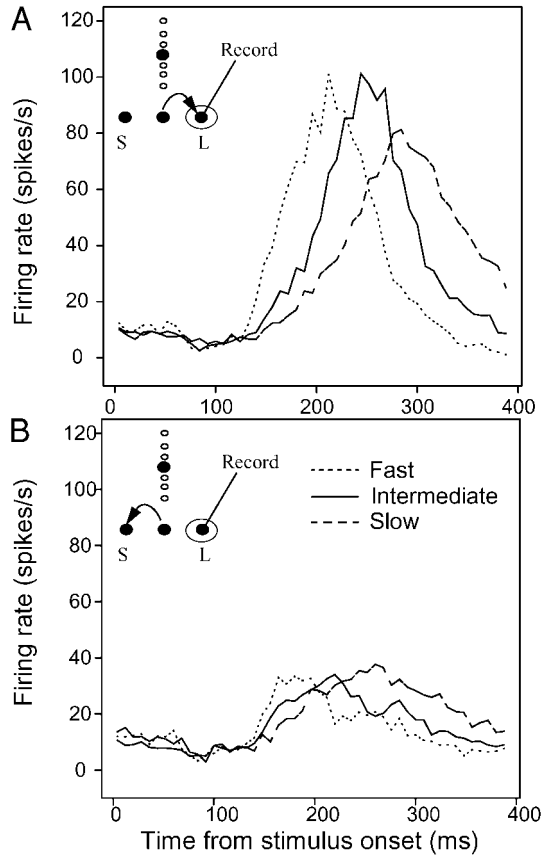

FIG. 9. Neural firing rates aligned on stimulus onset for fast, intermediate, and slow responses to medium stimuli (5 and 6°). Functions in *A* show the cell activity when a saccade was made to the target light in the cell's receptive field, and functions in *B* show the cell activity when a saccade was made to the other target light, the one not in the cell's receptive field. "Large" responses for recordings from cells with receptive field corresponding to the "large" response target (left colliculus) were combined with "small" responses for recordings from cells with receptive field corresponding to the "small" response target (right colliculus) for *A*. For *B*, "small" responses when recording from the "large" target were combined with "large" responses when recording from the "small" target. The 3 functions (the dotted, solid, and dashed lines) show responses for stimulus conditions divided into those with the shortest, intermediate, and longest reaction times according to the behavioral data. Cell activity is aligned to the onset of the stimulus light at time = 0 ms. Number of trials for each function in *A* is 577 and for *B* is 627 (3,612 of 15,453 trials for the 28 buildup cells in our experiment).

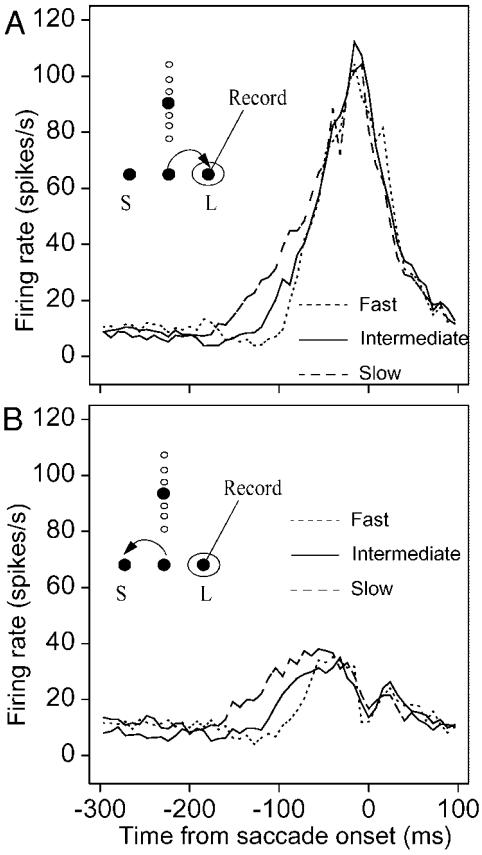

FIG. 10. Neural firing rates aligned on the saccade for fast, intermediate, and slow responses to medium stimuli (5 and 6°). Data and groupings are the same as in Fig. 9. The only difference is that the firing rate data are aligned on the saccade.

intermediate responses than for slow responses. The peak activity is about the same for firing rates for fast and intermediate responses (about 100 spikes/s) but is a little lower for slow responses (80 spikes/s). For firing rates for cells in the receptive field of a response target when the saccade is made to the other response target, the firing rates again start to rise at about the same point in time, and grow more quickly for fast responses than intermediate responses, and more quickly for intermediate responses than for slow responses. The functions grow to a much lower level than in Fig. 9*A*; about 30 spikes/s as opposed to 100 spikes/s.

Figure 10 shows the same firing rate data as in Fig. 9, but it is aligned on the saccade initiation. Although Sato et al. (2001) found no difference in the onset of discriminative information for firing rates aligned on the saccade as a function of the speed of the behavioral response, Hanes and Schall (1996) found different rates of increase in firing rate as a function of the reaction time for the saccade. However, Hanes and Schall presented data for responses for saccades into the receptive field of the target and not data for firing rates when the saccade was made to another target. Figure 10*A* shows firing rates for saccades into the receptive field of the response target, and Fig. 10*B* shows firing rates for the receptive field of a response target when the saccade is made to the other response target. Figure 10*A* shows differences in onset of the increase in firing rate and different rates of growth to peak activity that is quite similar to the pattern of results in Hanes and Schall (1996, their Fig. 3). However, Fig. 10*B* shows similar differences in the initial onset and initial growth in firing rates for cells in the receptive field of a response target when the saccade is made to the other response target.

Growth of discriminative information in firing rates

We can estimate the growth of discriminative information as in Sato et al. (2001) by subtracting the firing rates for Figs. 9, *A* and *B*, and 10, *A* and *B*. These are shown in Figs. 11*B* and 12*B*. Figure 11*B* shows that there is delayed onset of the firing rate for fast, intermediate, and slow responses. The differences in the initial rises for Fig. 9, *A* and *B*, cancel each other out, leading to a delay of about 40 ms between the firing rate functions for fast and intermediate responses and about 80 ms between the firing rate functions for fast and slow responses qualitatively replicating the results in Sato et al. (2001, their Fig. 3). In contrast, for responses aligned on the saccade (Fig. 12*B*), there is less than a 10 ms difference in the onset of the rise of discriminative information in firing rates for fast, intermediate, and slow responses. These functions are the targets for modeling by the diffusion model and the gray lines are fits of the diffusion model which will be discussed later.

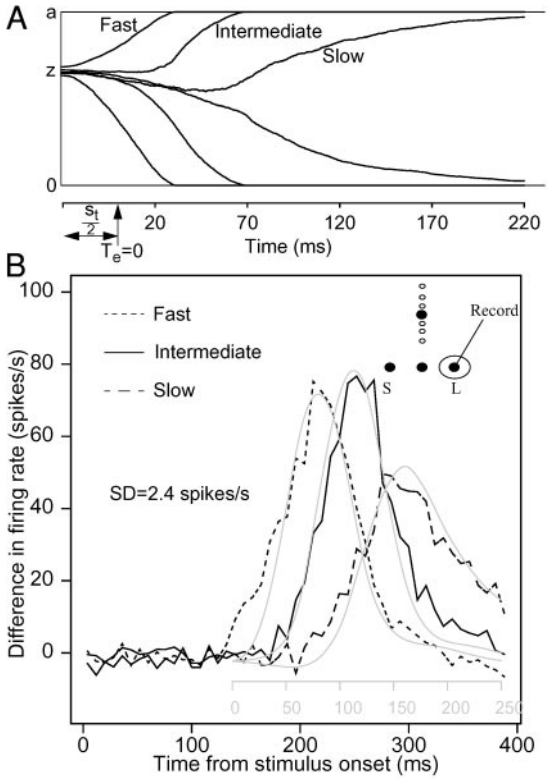

FIG. 11. Comparison of diffusion model predictions to differences in firing rates for fast, intermediate, and slow responses to medium stimuli aligned on the stimulus. *A*: average paths in the diffusion process for fast, intermediate, and slow responses derived from the parameter values for the fits of the model to the behavioral data in Fig. 6. These are the average of the average paths for the predictions from the parameter values for the 2 monkeys. Zero time is the first point in time at which diffusion processes can begin, and it corresponds to $T_e - s_t/2$. Black firing rate functions in *B* are the differences in firing rates obtained from the data in Fig. 9 by subtracting the functions in *B* from *A*. Gray lines in *B* are the differences in position between the paths for the "large" and "small" responses obtained from *A*. It is assumed that once a process hits the boundary in *A*, it exponentially decays back to the starting point with a decay constant of 20 ms.

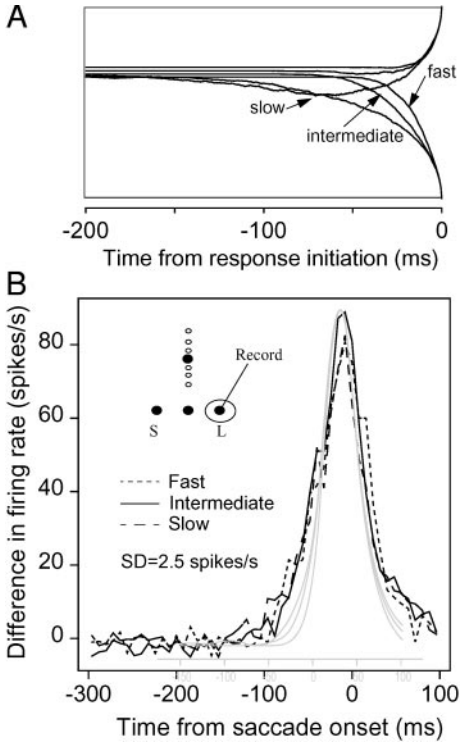

FIG. 12. Difference in firing rates for fast, intermediate, and slow responses to medium stimuli aligned on the saccade and diffusion model predictions. *A* and *B* are analogous to Fig. 11, *A* and *B*, except that the functions are aligned on the saccade instead of the stimulus. Firing rate functions are differences between firing rates displayed in Fig. 10, *A* and *B*.

Growth of discriminative information in the diffusion model

In this section, we present predictions for the growth of information prior to a decision in the diffusion model using the parameters obtained from fits of the model to the behavioral data. We compared these functions to the firing rate functions (Figs. 11 and 12) to determine whether the model makes the correct qualitative and quantitative predictions. The strength of this modeling endeavor is that the shapes and relative locations of the functions that describe the growth of discriminative information in the diffusion model are determined by parameters derived from fits of the model to the behavioral data; they are not derived from fitting the firing rate functions directly.

To obtain predictions from the diffusion model for the growth of discriminative information, we simulated 2,000 diffusion processes (Ratcliff and Tuerlinckx 2002) to produce simulated paths using parameters from the fits to the behavioral data (Tables 1 and 2). The drift rates for the 5 and 6° stimulus conditions (probability of a "large" response between 0.29 and 0.68, averaging about 0.5) were used because these were the two conditions used to generate the firing rate data in Figs. 11 and 12. The predictions presented in Figs. 11 and 12 were an average of the predictions from the parameter values from the two monkeys weighted according to the number of observations for each monkey in the data. We divided the simulated diffusion model paths based on the decision time into fast, intermediate, and slow thirds. The paths were aligned on the stimulus (Fig. 11) and on the decision (Fig. 12).

Figure 11*A* shows the average paths of the diffusion process for the fast third, the intermediate third, and the slow third of responses aligned on stimulus onset. The functions start at a point in time at which the first decision processes begin, which is $T_e - s_t/2$, where T_e is the component of T_{er} that represents encoding processes that precede the decision process. The functions show delays in discrimination between the three functions that match the delays observed in the data; the intermediate functions begin to separate 30 ms later than the fast functions, and the slow functions begin to separate 70 ms later than the fast functions. This predicted delay in discrimination is surprising because the diffusion model, which assumes a continuous growth of evidence, might be expected to show growth in discriminative information starting at the same point in time with different rates of separation (see also Ratcliff 1988). The delayed onset can be explained as follows: if a process has not terminated by, say 50 ms, it has to have remained between the two boundaries prior to this point. Because the accumulation process is very noisy, processes that are slow in terminating have an average position that lies in the middle between the two boundaries. For these parameter values, the prediction is that the average separation is close to zero for processes that eventually hit one boundary versus those that hit the other boundary.

We assumed that information that discriminates between the two responses is represented by the difference in position between the average paths for the two responses. If we plot the distance between the average paths, we obtain functions that grow from zero separation to a separation a, which is the distance between the two boundaries. Neuronal firing rate functions decay after the decision is made, so to model decay, we assumed that once the decision process hits the decision boundary, it exponentially decays back to the starting point. We found that a time constant of 20 ms was sufficient to produce predictions that mimic the observed decay in firing rates.

The gray smooth lines superimposed on the firing rate functions in Fig. 11*B* are predictions from the diffusion model from Fig. 11*A* for the average separation of the processes with decay back to the starting point after the process hits a decision boundary. To align the predicted function on the experimental data in Fig. 11*B*, the component of T_{er} prior to the mean start of the decision time (T_e) is estimated to be 142 ms and the mean time after the decision (T_r) is estimated to be 56 ms. The value of the height of the functions is 80 spikes/s, and the exponential decay time constant is 20 ms (i.e., by 20 ms after a process has hit the boundary, it has decayed about two-thirds of the way back to the starting point). The slow peak is lower than the fast and intermediate peaks because slow processes terminate over a wider range of stopping times than fast and intermediate processes. This means at any point after processes start to terminate, for slow processes relative to fast and intermediate processes, a greater proportion of processes are further away from the decision boundary either prior to terminating or during decay back to the starting point.

It should be stressed that apart from decay, time alignment of the functions and vertical scaling, the shapes, differences in onsets, relative peak heights, and relative decays are derived from the fits of the diffusion model to the behavioral data alone. It is also important to note that sources of variability in firing rates, e.g., in the onsets of firing rates across trials or blocks of trials, are also represented as sources of variability in the diffusion model by variability in diffusion model parameters across trials. Thus such sources of variability are present in

both the behavioral data, the firing rate data, and in the diffusion model.

Figure 12, *top*, shows diffusion model paths from the same simulations as in Fig. 11, but aligned on the decision. To produce the predicted functions, we added about one-half the variability in T_{er} (half s_t) to the predictions; this assumption corresponds to assuming part of the variability in processes other than the decision process comes from processes following the decision process. The main result is that the point at which the functions in Fig. 12*A* diverge does not differ much between the fast, intermediate, and slow thirds of the data. This is seen more clearly in the functions representing the difference in position, which are the gray smooth lines plotted in Fig. 12*B*. These functions diverge a little in their leading edges before they have reached 10 spikes/s, but the size of the difference is about the same as the initial noise in the empirical firing rate functions. The parameters for the alignment are peak activity of 85 spikes/s, a decay time constant of 20 ms, and a delay of 48 ms (T_r) after the decision before the response is initiated.

The result in Fig. 11 shows that discrimination is delayed for slow and intermediate responses relative to fast responses, but the data in Fig. 9 show about the same onsets in firing rates for fast, intermediate, and slow responses for saccades into the receptive field of the cell and also for saccades to the other target. In the diffusion model, equivalent onset times in Fig. 9 would be produced by individual processes moving away from the average paths shown in Fig. 11*A* and producing evidence toward one of the two alternatives (even though there is no difference in the average evidence). The same explanation holds for the two functions in Fig. 10 and the predictions and differences in Fig. 12, i.e., individual processes move away from the starting point earlier prior to the response for slow responses than fast responses and this corresponds to increased firing rates for both alternatives, but the average paths do not diverge earlier prior to the response for slow responses than fast responses which corresponds to discriminative information being available at about the same time.

Besides the cell activity corresponding to the decision process, a secondary result appears in the behaviors of the firing rates just prior to the rise in activity (Segraves et al. 1999). In most cells, there is a dip in activity of about 30% in the baseline firing rate 80–100 ms after stimulus onset followed by a rise back to the base firing rate just before the abrupt rise in firing rate that we attribute to the decision process (see Fig. 8, *A* and *B*). This dip is more pronounced in some cells than others and is present even in other classes of cells that appear to respond primarily to the presence of visual targets in their receptive fields. We conjecture that this dip in the firing rate corresponds to a global signal that something important is about to happen and this results in a global suppression of activity. In support of this proposal, a similar dip in activity has recently been reported for FEF neurons (Sato and Schall 2001).

The predictions from the diffusion model do not match the firing rate data perfectly in Figs. 11 and 12. SD in the firing rates was computed from the period of firing prior to the point where the functions begin to rise, and for Figs. 11 and 12, these were both 2.5 spikes/s (which means differences >5 spikes/s are significant). These estimates underestimate variability in higher firing rates (cf., Mazurek and Shadlen 2002), but can serve as a conservative estimate, i.e., differences between predicted and experimental firing rates at a single point in time <5 spikes/s are probably not significant, but, of course, systematic differences across several points in time of a size <5 spikes/s can be significant. In Fig. 11, the firing rate function for the fastest third of responses begins to rise 20 ms earlier than the predicted function and rises less steeply than the predictions. However, by the time the difference in firing rates reaches 20 spikes/s, the functions coincide. Decay in the firing rate function for the intermediate third of responses is a little slower than the prediction. Two of the parameters added to the diffusion model to produce the predictions to match the firing rate functions, the mean time from the decision to the response and peak activity, differ for functions aligned on the stimulus and the saccade. The difference is about 10 ms in the estimate of the decision to response time and about 5 spikes/s in the activity. This is because the diffusion model predicts a slightly faster decision process with greater variability in parameters across trials than is required for it to match the firing rate data. This would account for the predicted functions for alignment on the saccade that are too narrow relative to the firing rate functions. Despite these discrepancies, the predicted functions match both the quantitative and qualitative trends well.

Growth of discriminative information in the Poisson counter model

We derived predictions from the Poisson counter model in the same way as for the diffusion model. Specifically, we generated 2,000 simulated processes from the Poisson counter model using the parameters for the best fit to the experimental data for monkey MK03. We used the average of the Poisson rates for the middle two stimulus conditions (Fig. 7, *C* and *D*). Because the two criteria could have different values, we computed the ratio of the number of counts divided by the criterion value (in 1 ms steps) in each counter to provide a measure of relative distance to the criterion. We subtracted these proportions from each another and used this difference to represent discriminative information in the model. When one of the processes hit its decision criterion, we assumed that both processes decayed back to zero with a time constant of 20 ms (the same one used for the diffusion model).

Figure 13 shows the growth of discriminative information as a function of fast, intermediate, and slow responses in the Poisson counter model aligned on the beginning of the decision process. The results show a gradual growth from a common point of onset that is quite unlike the data or the predictions from the diffusion model (Fig. 11). The interpretation of this gradual growth is that as evidence grows in one counter, it also grows in the other counter, but at a lower rate. This means that the difference begins to grow at the same point in time for fast, intermediate, and slow responses as is shown in Fig. 13.

The Poisson counter model shows a gradual rise because the accumulation of evidence in the two counters is not competitive. This means that evidence for both alternatives gradually grows independently of each other. In contrast, the diffusion model implements competition because evidence toward one alternative is evidence against the other (a step toward one decision boundary is a step away from the other decision boundary).

We believe that the delayed onset of discriminative information in firing rates can be predicted by some (e.g., Ornsetin Uhlenbeck models, see Ratcliff and Smith 2003) but not all

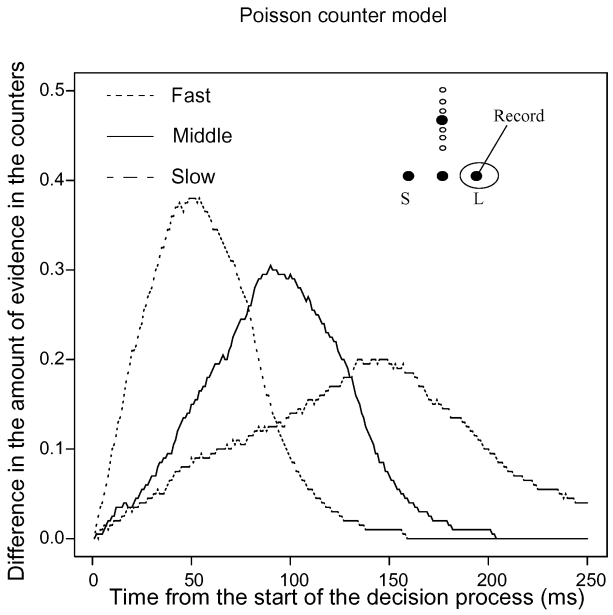

FIG. 13. Growth of discriminative information in the Poisson counter model. Two thousand simulated Poisson counter processes were generated from the Poisson counter model using the average accrual rate for stimuli 5 and 6° for Monkey MK03. The difference in the proportion of counts (relative to the criterion for that counter) between the two counters is plotted for fast, intermediate, and slow responses.

sequential sampling models. It is likely that models like the Poisson counter model that use two counters and absolute decision criteria, such as the accumulator and recruitment models (see Ratcliff and Smith 2003), predict the same pattern of growth of discriminative information as the Poisson counter model.

In one sense, the Poisson counter model could be seen as a straw man because it does not fit the data. However, when we began applying the model, we had no idea whether it would succeed or fail. In fact, the explanations for the onset of discriminative information for the diffusion and Poisson counter models (Figs. 11 and 13) were produced only after obtaining predictions from the models.

DISCUSSION

Our results provide three main findings. First, the diffusion model, developed in the human behavioral domain, fits the monkey behavioral data well and in ways similar to human data. Second, single cell firing rate data aligned on either stimulus onset or response initiation (saccade initiation) match the time course of accumulation of evidence in the diffusion model predicted using parameter values derived from the fits to behavioral data. Third, both the behavioral data and the neural firing rate data are not fitted by the Poisson counter model which shows that both behavioral data and the neural firing rate data discriminate between the predictions from the behavioral models.

Ratcliff and Smith (2003) examined the ability of several sequential sampling models to mimic each other. They found that the diffusion model and the Poisson counter model do not mimic each other. The Poisson counter model fails to fit predictions from the diffusion model in ways similar to the discrepancies between the Poisson counter model and the data shown in Fig. 7 above. The Poisson counter model produces almost flat quantile probability functions with a slight increase as probability values decrease to the left (showing that "error" reaction times are longer than correct reaction times). The diffusion model predicts functions that are inverted U-shaped. The reaction time distributions for the Poisson counter model are predicted to be more normal than the data and also more normal than those predicted from the diffusion model. This can be seen in the larger predicted spread between the 0.1 and 0.3 reaction time quantiles for the Poisson counter model compared with the diffusion model. The Poisson counter model also fails to fit the leading edge of the reaction time distribution. The results presented here show that the diffusion model fits the behavioral data, but the Poisson counter model does not.

We designed our task so that the stimulus dimension (separation of 2 stimulus lights) does not directly map into the same representation in the response system (i.e., the SC). This reduces the likelihood that information from early visual representations can be passed through to the output to facilitate the response in the absence of decision making about the stimulus. Likewise, the response targets in our task were continually illuminated, eliminating the possibility of effects of response target onset on a cell's activity. In our task, processing requires a transformation between the stimulus and response. The nature of representations and processing that are involved in making such simple decisions is one of the most important problems in psychology and neuroscience. In our modeling, about 200 ms of processing time is not involved in the decision process and from the neural firing rate data, about 150 ms is involved in processes prior to the decision process, and about 50 ms involved in processes after the decision process. The 150 ms of processing time prior to the decision process in our view is involved in stimulus encoding and mapping the representation of the stimulus to the decision process based on the response dimension.

Model flexibility

A common criticism of behavioral models of the complexity of these sequential sampling models for reaction time reduces to the question: "With 8 or 10 parameters, can you fit any pattern of data?" The short answer is no. Roberts and Pashler (2000) raised this issue in discussing how to evaluate models. They argued that to evaluate a successful model, it is just as important to know what a model cannot fit as it is to know what a model can fit; if a model can fit any possible pattern of data, it could be considered as a summary of data, but little more. Ratcliff (2002) addressed this issue for the diffusion model by making up a number of plausible patterns of data and then showing that the diffusion model was unable to fit them. Examples included normally distributed reaction time distributions, reaction time distributions with tails longer than the exponential distribution, quantile probability functions with the distributions shifting across probability conditions instead of spreading as reaction time increased, U-shaped (instead of inverted U-shaped) quantile probability functions, and so on. In each of these cases, the diffusion model produced substantial discrepancies between the fake data set and predictions. Thus the diffusion model, even with its many parameters, is extremely constrained and only seems to fit patterns of data that

are obtained from both experiments with human subjects and from this experiment.

Deterministic decision models

To evaluate the claim that the prelude/buildup cells in the SC (and the movement sensitive cells in the FEF) are implementing the behavioral decision process, we need to examine alternative views. It may be thought that the prelude/buildup of activity is stereotypical and does not reflect the decision process. One specific implementation of this view might be the LATER model (Reddi and Carpenter 2000, 2001; see also Cook and Maunsell 2002). In this model, activity is built up deterministically in a counter toward a decision criterion. The main aim of the model was to account for the shape of reaction time distributions. In the model, variability in reaction times comes about because the rate of accumulation of evidence varies across trials (cf., variability in drift rate across trials in the diffusion model). The LATER model, however, does not deal with the important relationship between speed and accuracy. Reaction time and accuracy covary in two ways in experimental data. First, subjects can trade speed and accuracy; in fact, large changes in reaction time, e.g., 200–400 ms in mean reaction time, are accompanied by modest changes in accuracy, e.g., 4–8% (see Ratcliff 2002; Ratcliff and Rouder 1998; Ratcliff et al. 2001). Second, given a particular speed-accuracy setting, manipulating the difficulty of the decision leads to changes in both accuracy and reaction time so that as accuracy improves, reaction time shortens. Because accuracy and reaction time have been found to covary in thousands of experiments with human subjects, models must be able to account for their joint behavior. In the experiment reported here, the LATER model cannot account for both "large" and "small" responses to large stimuli (and both "large" and "small" responses to small stimuli), nor does it account for the probability of each response type.

If, as Reddi and Carpenter (2001) propose, the decision between the two alternatives is made at a different location from the process that accumulates evidence to produce the reaction time, then there can be no speed-accuracy tradeoff as a result of changing the decision criterion. If the decision criterion is reduced in the LATER model, there is no effect on accuracy, only reaction time is reduced. In fact, no matter how much the criterion is reduced, accuracy stays the same, so there is no need in the model to set the criterion at any value except the smallest possible. The LATER model account would also produce no growth of accuracy in experimental paradigms in which subjects are required to respond at experimenter determined times in the response signal procedure (e.g., Dosher 1976; Ratcliff 1978; Reed 1976; Wickelgren 1977). This is because the growth of evidence is deterministic in the model, and accuracy does not change as a function of time. Other deterministic models, such as the "winner take all network" discussed in Wilson (1999) have the same kinds of problems because they cannot represent the growth of evidence over time.

Another possibility is that the output of a decision system earlier in the processing stream sends its output to the prelude/buildup cells in the SC and movement-related cells in the FEF and these simply track the output of this earlier system. If this view of processing were correct, then our analyses would apply to this earlier decision process (cf., Cook and Maunsell 2002).

Alternative stochastic decision models

Another question is how constraining are both the behavioral data and the neural data for models of processing? We were able to answer this question by fitting another model for reaction time, the Poisson counter model, to the behavioral data and then generated predictions for growth of discriminating information. The fits to the behavioral data were not particularly good as noted earlier, and there were significant discrepancies between the best fits and the data. In addition, the growth of discriminative information aligned on the beginning of the decision process did not show the delayed onset for slow relative to intermediate, and intermediate relative to fast decisions as was obtained for both the diffusion model and for the firing rate data. Thus we can say that the delayed onset of discriminative information is not a pattern that is predicted by all stochastic models of evidence accumulation.

Neural plausibility

The diffusion model does not align naturally with what we know about the neural populations that we assume to be implementing the decision. The diffusion model assumes that evidence is accumulated in one counter so that evidence for one alternative is evidence against the other alternative. Gold and Shadlen (2001) present an analysis designed to show how a diffusion model could be neurally implemented. They assumed coupled pairs of populations of neurons that are negatively correlated so that an increase in firing rate in one population corresponds to a decrease in the other. This implements competition that is needed to mimic the diffusion model. In contrast, the Poisson counter model assumes two counters that race each other, that might be implemented as two populations of neurons (for our task) such as the populations of neurons corresponding to the two decisions in the SC or FEF.

In the behavioral modeling domain, there are two new models that mimic the diffusion model and have two counters that compete against each other just as in the Poisson counter model. One is the leaky competing accumulator model of Usher and McClelland (2001), and the other is the leaky accumulator with relative criterion (Ratcliff and Smith 2003). As activation builds up in the models, decay or leakage serves to limit activation so it cannot grow indefinitely. In the Usher and McClelland model, the two counters inhibit each other so the greater the activation in one counter, the more it inhibits the other. This would require the neural populations that implement the decision to project to each other either directly or indirectly and explicitly inhibit each other. The leaky accumulator with relative criterion is more closely related to the two counter implementation of the diffusion model described above. It uses a relative decision criterion as in the diffusion model instead of inhibition between counters used in the Usher and McClelland model to produce competitive behavior. Ratcliff and Smith (2003) have shown that both of these models mimic the diffusion model in fitting several highly constrained experiments. At this point in the evolution of these models, the similarities between the models are much greater than the differences and we might view the three models as different

ways of implementing a competitive or relative decision rule. As can be seen from the contrast between the diffusion model and the Poisson counter model, the key property that allows the diffusion model to fit the neural data are the competition between the two responses as implemented as a relative decision stopping rule or as competition between pools of neurons.

Figure 8*B* provides results that can be interpreted as competition within the theoretical frameworks of the competing accumulator models. When the probability of making a "large" response is high, but a "small" response is made, the firing rate is higher in neurons corresponding to the "large" response than when the probability of making a "large" response is low and a "small" response is made. In the Usher and McClelland model, this would be explained by a higher accrual rate toward a "large" response when the probability of making a "large" response is high than when the probability of making a "large" response is small. Inhibition would reduce the activity more in the latter case than the former case. In the relative criterion accumulator, the explanation is different. When a process terminates, the difference in evidence between the two counters is the same value for all processes. However, the results are averaged over a range of finishing times, so the activity in the counter to which the response is not made will have an average lower absolute level when the accrual rate is lower than when the accrual rate is higher.

Competing activity or comparisons necessary for the relative criterion models could result from interactions taking place within the SC as well as between colliculi in the left and right hemispheres. Intrinsic as well as commissural projections of collicular neurons exist that could form a substrate for such competition or comparisons (Moschovakis et al. 1988, 1996; Munoz and Istvan 1998). It is also possible that competition could take place between upstream sites that project to the SC. Because the rise in activity coincides for the cells corresponding to the two targets, there is no evidence for a shift in activity from one colliculus to the other.

Roitman and Shadlen (2002) present data from a motion discrimination task in which neural recordings were obtained from the lateral interparietal (LIP) area. The data presented are similar to those presented in this article with the exception that in Roitman and Shadlen's data, the firing rates have a high initial value and activity rises when the response is made into the cell's receptive field and falls when the response is made to the other response target. The rise and fall are more extreme for strong than weak stimuli. Our results show all cells have activity that begins at a low baseline level which increases, with more activity in the cells that correspond to the target light to which the response is not made when the response to that target light is more probable.

The LIP may be part of the same circuit as the SC, and so activity in these and the FEF may all be implementing the decision process (or one area may be mainly responsible). However, it is known that the LIP is more concerned with the visual stimulus than the response. For example, Pare and Wurtz (2001) found that activity in the LIP depended on the sustained presence of the visual stimulus while activity in the SC did not.

Roitman and Shadlen (2002) argue for a similar evidence accumulation process to that presented in this article. We hope that the new models can be applied to data such as those presented by Roitman and Shadlen and account for patterns like theirs and like those presented here.

By themselves, the neurophysiological results reported here mirror the results reported previously by other laboratories. A number of earlier studies have demonstrated a positive correlation between the level of collicular buildup cell activity and increasing likelihood (Dorris and Munoz 1998; Dorris et al. 2000) as well as decreasing latency of a saccade into the activity field of the cell (Basso and Wurtz 1998; Dorris et al. 2000; Everling et al. 1999). In addition, significant effects of target and reward probability on the activity levels of collicular buildup cells as well as cells in the LIP have also been reported (Basso and Wurtz 1998; Platt and Glimcher 1999). The emphasis of our report is to extend those findings by the direct application of a well developed decision model to the eye movement behavior and collicular buildup cell activity observed in a two-choice task.

In this article, model simulations were based on the average of many successive simulations of the diffusion process. Developing a model that was truly neurally plausible would involve implementing a diffusion process, or a process that mimicked the diffusion process, using a large number of units representing prelude/buildup cells running in parallel. When a decision was made by this system, the cells would produce activation within the superior colliculus (and perhaps in circuits involving the LIP and FEF) as well as in collicular targets within downstream oculomotor regions of the brain stem that implement the response based on the behavioral decision. The approach of this article is to begin with the behavioral data and work backward through behavioral models to try to describe the neural data. We hope that this approach will dovetail with approaches that begin with the neural processing data and work toward the behavioral data.

The challenge presented by this research is to understand what the neural decision rule is. Clearly, a decision is taken when one population of neurons tells another population to produce a response, but the precise signal is unknown. For example, the signal could be a particular number of cells firing within a short period of time, a specified number of spikes being produced within a certain time in a critical area, or any of a variety of other possibilities. However, no matter what the exact signal is, the success of the diffusion model in fitting the behavioral data and its agreement with the neural firing data point to the possibility of closer theoretical integration of neural data and behavioral data through the implementation of well developed stochastic models that can be applied in both domains (cf. Gold and Shadlen 2001; Hanes and Schall 1996).

We thank Gail McKoon for extensive comments on this article and Angela Nitzke and the staff of Northwestern's Center for Experimental Medicine for animal care; Northwestern's Instrument and Electronics Shops for machining and electronic hardware. We also thank Mark Depristo, Usman Muzaffer, and T. J. Bay for programming assistance.

DISCLOSURES

This article was supported by National Institutes of Health Grants R01-MH-59893, R37-MH-44640, R01-EY-08212, and K05-MH-01891.

REFERENCES

Ashby FG. A stochastic version of general recognition theory. *J Math Psych* 44: 310–329, 2000.

Basso MA and Wurtz RH. Modulation of neuronal activity in superior colliculus by changes in target probability. *J Neurosci* 18: 7519–7534, 1998.

Bichot NP, Thompson KG, Rao SC, and Schall JD. Reliability of macaque frontal eye field neurons signaling saccade targets during visual search. *J Neurosci* 21: 713–725, 2001.

Busemeyer JR and Townsend JT. Decision field theory: a dynamic-cognitive approach to decision making in an uncertain environment. *Psychol Rev* 100: 432–459, 1993.

Cook EP and Maunsell JHR. Dynamics of neuronal responses in macaque MT and VIP during motion detection. *Nat Neuro* 5: 985–994, 2002.

Cynader M and Berman N. Receptive-field organization of monkey superior colliculus. *J Neurophysiol* 35: 187–201, 1972.

Dias EC and Segraves MA. Muscimol-induced inactivation of monkey frontal eye field: effects on visually and memory-guided saccades. *J Neurophysiol* 81: 2191–2214, 1999.

Dorris MC and Munoz DP. Saccadic probability influences motor preparation signals and time to saccadic initiation. *J Neurosci* 18: 7015–7026, 1998.

Dorris MC, Pare M, and Munoz DP. Immediate neural plasticity shapes motor performance. *J Neurosci* 20: 1–5, 2000.

Dosher BA. The retrieval of sentences from memory: a speed-accuracy study. *Cogn Psych* 8: 291–310, 1976.

Everling S, Dorris MC, Klein RM, and Munoz DP. Role of primate superior colliculus in preparation and execution of anti-saccades and pro-saccades. *J Neurosci* 19: 2740–2754, 1999.

Glimcher PW and Sparks DL. Movement selection in advance of action in the superior colliculus. *Nature* 355: 542–545, 1992.

Gold JI and Shadlen MN. Representation of a perceptual decision in developing oculomotor commands. *Nature* 404: 390–394, 2000.

Gold JI and Shadlen MN. Neural computations that underlie decisions about sensory stimuli. *Trends Cogn Sci* 5: 10–16, 2001.

Hanes DP and Schall JD. Neural control of voluntary movement initiation. *Science* 274: 427–430, 1996.

Horwitz GD and Newsome WT. Separate signals for target selection and movement specification in the superior colliculus. *Science* 284: 1158–1161, 1999.

Horwitz GD and Newsome WT. Target selection for saccadic eye movements: prelude activity in the superior colliculus during a direction-discrimination task. *J Neurophysiol* 86: 2543–2558, 2001.

Kim JN and Shadlen MN. Neural correlates of a decision in the dorsolateral prefrontal cortex of the macaque. *Nature Neurosci* 2: 176–185, 1999.

Krauzlis RJ and Dill N. Neural correlates of target choice for pursuit and saccades in the primate superior colliculus. *Neuron* 35: 355–363, 2002.

LaBerge DA. A recruitment theory of simple behavior. *Psychometrika* 27: 375–396, 1962.

LaBerge DA. Quantitative models of attention and response processes in shape identification tasks. *J Math Psych* 38: 198–243, 1994.

Luce RD. *Response Times.* New York: Oxford, 1986.

Mays LE and Sparks DL. Dissociation of visual and saccade-related responses in superior colliculus neurons. *J Neurophysiol* 43: 207–232, 1980.

Mazurek ME and Shadlen MN. Limits to the temporal fidelity of cortical spike rate signals. *Nat Neurosci* 5: 463–471, 2002.

Mohler CW and Wurtz RH. Organization of monkey superior colliculus: intermediate layer cells discharging before eye movements. *J Neurophysiol* 39: 722–744, 1976.

Moschovakis AK, Karabelas AB, and Highstein SM. Structure-function relationships in the primate superior colliculus. II. Morphological identity of presaccadic neurons. *J Neurophysiol* 60: 263–302, 1988.

Moschovakis AK, Scudder CA, and Highstein SM. The microscopic anatomy and physiology of the mammalian saccadic system. *Progress Neurobiol* 50: 133–254, 1996.

Munoz DP and Istvan PJ. Lateral inhibitory interactions in the intermediate layers of the monkey superior colliculus. *J Neurophysiol* 79: 1193–1209, 1998.

Munoz DP and Wurtz RH. Saccade-related activity in monkey superior colliculus. I. Characteristics of burst and buildup cells. *J Neurophysiol* 73: 2313–2333, 1995.

Nosofsky RM and Palmeri TJ. An exemplar based random walk model of speeded classification. *Psychol Rev* 104: 266–300, 1997.

Pare M and Wurtz RH. Progression in neuronal processing for saccadic eye movements from parietal cortex area LIP to superior colliculus. *J Neurosci* 22: 2545–2562, 2001.

Pike AR. Stochastic models of choice behaviour: response probabilities and latencies of finite Markov chain systems. *Br J Math Stat Psychol* 21: 161–182, 1966.

Pike R. Response latency models for signal detection. *Psychol Rev* 80: 53–68, 1973.

Platt ML and Glimcher PW. Neural correlates of decision variables in parietal cortex. *Nature* 400: 233–238, 1999.

Ratcliff R. A theory of memory retrieval. *Psychol Rev* 85: 59–108, 1978.

Ratcliff R. Group reaction time distributions and an analysis of distribution statistics. *Psychol Bull* 86: 446–461, 1979.

Ratcliff R. A theory of order relations in perceptual matching. *Psychol Rev* 88: 552–572, 1981.

Ratcliff R. Continuous versus discrete information processing: modeling the accumulation of partial information. *Psychol Rev* 95: 238–255, 1988.

Ratcliff R. Putting noise into neurophysiological models of simple decision making. *Nat Neurosci* 4: 336, 2001.

Ratcliff R. A diffusion model account of reaction time and accuracy in a brightness discrimination task. *Psychol Bull Rev* 9: 278–291, 2002.

Ratcliff R, Gomez P, and McKoon G. Diffusion model account of lexical decision. *Psychol Rev* In press.

Ratcliff R and Rouder JN. Modeling response times for two-choice decisions. *Psychol Sci* 9: 347–356, 1998.

Ratcliff R and Rouder JN. A diffusion model account of masking in letter identification. *J Exp Psychol Hum Percept Perform* 26: 127–140, 2000.

Ratcliff R and Smith PL. A comparison of sequential sampling models for two-choice reaction time. *Psychol Rev* In press.

Ratcliff R, Thapar A, and McKoon G. The effects of aging on reaction time in a signal detection task. *Psychol Aging* 16: 323–341, 2001.

Ratcliff R and Tuerlinckx F. Estimating the parameters of the diffusion model: approaches to dealing with contaminant reaction times and parameter variability. *Psych Bull Rev* 9: 438–481, 2002.

Ratcliff R, Van Zandt T, and McKoon G. Connectionist and diffusion models of reaction time. *Psychol Rev* 106: 261–300, 1999.

Reddi BA and Carpenter RH. The influence of urgency on decision time. *Nat Neurosci* 3: 827–830, 2000.

Reddi BA and Carpenter RH. Putting noise into neurophysiological models of simple decision making. *Nat Neurosci* 4: 337, 2001.

Reed AV. List length and the time course of recognition in human memory. *Mem Cogn* 4: 16–30, 1976.

Roberts S and Pashler H. How persuasive is a good fit? A comment on theory testing. *Psychol Rev* 107: 358–367, 2000.

Robinson DA. Eye movements evoked by collicular stimulation in the alert monkey. *Vision Res* 12: 1795–1808, 1972.

Roe RM, Busemeyer JR, and Townsend JT. Multialternative decision field theory: a dynamic connectionist model of decision-making. *Psychol Rev* 108: 370–392, 2001.

Roitman JD and Shadlen MN. Responses of neurons in the lateral interparietal area during a combined visual discrimination reaction time task. *J Neurosci* 22: 9475–9489, 2002.

Rouder JF and Ratcliff R. Comparing categorization models. *J Exp Psychol General* In press.

Sato T and Schall JD. Pre-excitatory pause in frontal eye field responses. *Exp Brain Res* 139: 53–58, 2001.

Sato T, Murthy A, Thompson KG, and Schall JD. Search efficiency but not response interference. *Neuron* 30: 583–591, 2001.

Schall JD, Hanes DP, Thompson KG, and King DJ. Saccade target selection in frontal eye field of macaque. I. Visual and premovement activation. *J Neurosci* 15: 6905–6918, 1995.

Segraves MA. Activity of monkey frontal eye field neurons projecting to oculomotor regions of the pons. *J Neurophysiol* 68: 1967–1985, 1992.

Segraves MA, Cherian A, and Ratcliff R. Rhesus monkey performance and superior colliculus activity during a reaction time task. *Soc Neurosci Abstr* 25: 1920, 1999.

Smith PL. Psychophysically principled models of visual simple reaction time. *Psychol Rev* 102: 567–591, 1995.

Smith PL and Van Zandt T. Time-dependent Poisson counter models of response latency in simple judgment. *Br J Math Stat Psychol* 53: 293–315, 2000.

Sparks DL. Conceptual issues related to the role of the superior colliculus in the control of gaze. *Curr Opin Neurobiol* 9: 698–707, 1999.

Sparks DL, Holland R, and Guthrie BL. Size and distribution of movement fields in the monkey superior colliculus. *Brain Res* 113: 21–34, 1976.

Swensson RG. The elusive tradeoff: speed versus accuracy in visual discrimination tasks. *Percept Psychophys* 12: 16–32, 1972.

Thompson KG, Hanes DP, Bichot NP, and Schall JD. Perceptual and motor processing stages identified in the activity of macaque frontal eye field neurons during visual search. *J Neurophysiol* 76: 4040–4055, 1996.

Townsend JT and Ashby FG. *Stochastic Modeling of Elementary Psychological Processes.* Cambridge, UK: Cambridge University Press, 1983.

Usher M and McClelland JL. The time course of perceptual choice: the leaky, competing accumulator model. *Psychol Rev* 108: 550–592, 2001.

Van Zandt T, Colonius H, and Proctor RW. A comparison of two response time models applied to perceptual matching. *Psychol Bull Rev* 7: 208–256, 2000.

Wickelgren WA. Speed-accuracy tradeoff and information processing dynamics. *Acta Psychologica* 41: 67–85, 1977.

Wilson HR. *Spikes, Decisions, and Actions: The Dynamical Foundations of Neuroscience.* New York: Oxford Univ Press, 1999.